Journal of NeuroVirology, 15: 211–218, 2009

ISSN 1355-0284 print / 1538-2443 online
DOI: 10.1080/13550280902913255

informa
healthcare

Nocodazole delays viral entry into the brain following footpad inoculation with West Nile virus in mice

EA Hunsperger,[1] and JT Roehrig[2]

[1]Centers for Disease Control and Prevention, Dengue Branch, San Juan, Puerto Rico; and [2]Centers for Disease Control and Prevention, Fort Collins, Colorado, USA

West Nile virus (WNV) infection in humans can cause neurological deficits, including flaccid paralysis, encephalitis, meningitis, and mental status change. To better understand the neuropathogenesis of WNV in the peripheral and the central nervous systems (PNS and CNS), we used a mouse footpad inoculation model to simulate a natural peripheral infection. Localization of WNV in the nervous system using this model has suggested two routes of viral invasion of the CNS: axonal retrograde transport (ART) from the PNS and hematogenous diffusion via a breakdown in the blood-choroid-plexus barrier. C57BL/6J mice were treated with nocodazole, a microtubule inhibitor that blocks ART, prior to infection with WNV. Nocodazole-treated WNV-infected mice developed a viremia 1.5 $\log_{10}$ greater than untreated WNV-infected control mice at days 3 to 4 post infection (PI). Although viremia was greater in nocodazole-treated mice, detection of virus in brain tissue (spinal cord, cortex, brainstem, and cerebellum), as measured by real-time reverse transcriptase–polymerase chain reaction (RT-PCR), did not occur until day 7. At these later time points (7 and 9 days PI), nocodazole-treated WNV-infected animals attained viral titers in these tissues similar to titers in the untreated WNV-infected control animals. These results demonstrate that a single dose of nocodazole delays, but does not block, WNV infection of the brain. *Journal of NeuroVirology* (2009) **15,** 211–218.

Keywords: flavivirus; mice; nocodazole; West Nile virus

Introduction

West Nile virus (WNV) is a member of the family *Flaviviridae* of the arthropod-borne positive-strand RNA viruses and was first isolated from a febrile woman in Uganda in 1937 (Smithburn *et al*, 1940). The virus is maintained in a natural cycle involving a mosquito vector and avian amplifying hosts, with humans as dead-end incidental host. WNV belongs to the Japanese encephalitis (JE) serocomplex of flaviviruses that also includes the medically important St. Louis encephalitis (SLE), Murray Valley encephalitis (MVE), and Kunjin viruses. Its genome consists of a single-stranded positive-sense RNA of approximately 11 kb in length that encodes a single open reading frame. The synthesized polyprotein is composed of both structural (envelope and capsid) and nonstructural proteins (NS1, NS2A, NS2B, NS3, NS4A, NS4B, and NS5). All of the nonstructural genes assist with viral RNA synthesis at some level (Brinton, 2002).

WNV first emerged as a public health threat in the United States in 1999 (Anderson *et al*, 1999; Lanciotti *et al*, 1999). During the initial outbreak, 62 cases were identified, of which 59 case-patients were hospitalized with encephalitis, meningitis, or flaccid paralysis and 7 died (Briese *et al*, 1999; Lanciotti *et al*, 1999; Nash *et al*, 2001). From 1999 to 2006, over 10,697 cases of WNV neuroinvasive disease have been identified (www.cdc.gov/ncidod/dvbid/westnile/index.htm). The diagnosis of flaccid paralysis in certain individuals prompted the use of the term

Address correspondence to Elizabeth A. Hunsperger, PhD, Center for Disease Control and Prevention (CDC), National Center for Infectious Diseases, Division of Vector-Borne Infectious Diseases, 1324 Calle Canada, San Juan, PR 00920, Puerto Rico. E-mail: enh4@cdc.gov

The authors would like to acknowledge Dr. Brad Biggerstaff and Luis Manuel Santiago for their assistance with the statistical analysis of the data.

Received 10 September 2008; revised 5 February 2009; accepted 2 March 2009

''poliomyelitis-like'' syndrome associated with WNV infection (Doron *et al*, 2003; Leis *et al*, 2003). In 2004, a more stringent case definition for WNV-neuroinvasive disease was established by the Centers for Disease Control and Prevention (CDC). The new case definition included the presence of fever and at least one of the following symptoms to better define the neurological aspect of the disease: (1) acutely altered mental status (e.g., disorientation, obtundation, stupor, or coma); 2) other acute signs of central or peripheral neurologic dysfunction (e.g., paresis or paralysis, nerve palsies, sensory deficits, abnormal reflexes, generalized convulsions, or abnormal movements); (3) pleocytosis (increased white blood cell concentration in cerebrospinal fluid [CSF]) associated with illness clinically compatible with meningitis (e.g., headache or stiff neck).

In our previous studies, we used *in vivo* mouse footpad inoculation to model the natural progression of WNV from the site of a mosquito bite to the central nervous system (CNS). These studies demonstrated the presence of WNV antigens in the dorsal root ganglion (DRG) neurons of the peripheral nervous system (PNS), suggesting that these WNV-infected neurons may contribute to the rapid introduction of the virus into the CNS via axonal retrograde transport (ART) (Hunsperger and Roehrig, 2005, 2006). Results from a subsequent hamster study supported this hypothesis (Samuel *et al*, 2007). The results of our current study using nocodazole, a microtubule inhibitor, provide additional evidence of the importance of ART to the pathogenesis of WNV in the mouse model. Mice treated with nocodazole prior to a peripheral WNV inoculation demonstrated a significant 6-day delay in viral infection of the CNS.

Results

Nocodazole treatment increased level but not duration of WNV viremia in mouse serum

The peak viremia in nocodazole-treated or untreated WNV-infected mice occurred on day 3 PI. Nocodazole-treated animals demonstrated 1.5 $\log_{10}$ higher peak viremia in the serum than untreated WNV-infected animals (analysis of variance [ANOVA] mixed model $P < .0001$) (Figure 1A, B).

Appearance of vRNA in the CNS was delayed by nocodazole treatment and overall WNV titers were greater than in untreated WNV-infected animals

The kinetics of WNV RNA accumulation in neural tissue differed between nocodazole-treated and untreated WNV-infected mice. Results from the spinal cord indicated that there were relatively small amounts of vRNA present during the first 4 days of nocodazole treatment. On the other hand, in the untreated WNV-infected mice, the vRNA was detected as soon as day 1 post-infection (PI) and throughout the early time points, with the highest activity at day 7 PI. Nocodazole treatment at day 7 PI resulted in an 1.16-fold increase of vRNA compared to untreated WNV-infected animals and this difference was statistically significant (Figure 2A, B; ANOVA mixed model $P = .01$).

In the brainstem, there was activity in the nocodazole-treated and the untreated WNV-infected animals early in the infection, at 1 day PI; however, in the nocodazole-treated animals, none of the other time points had vRNA present (2 to 4 days). On day 7 PI, there was an increase in vRNA in the nocodazole-treated animals, with a $>4 \log_{10}$ difference compared to the untreated WNV-infected animals. On day 9 PI, there was a $>2 \log_{10}$ difference between the two samples, with the nocodazole treatment presenting with higher levels of vRNA when compared to the untreated WNV-infected animals (Figure 2C, D).

In the cerebellum, the nocodazole-treated animals had vRNA detectable as early as day 1 PI, which disappeared for the next 3 days, similar to the brainstem. At day 7 PI, there was a 5.4 $\log_{10}$ increase in vRNA in the nocodazole-treated versus the untreated WNV-infected animals. This vRNA decreased slightly for nocodazole-treated animals and the difference between the untreated WNV-infected and nocodazole-treated animals on day 9 PI was 1.7 $\log_{10}$ (Figure 2E, F).

Interestingly, vRNA was not present in the cortex during the early time points, from 1 to 4 days PI, in the nocodazole-treated animals. However, activity was observed in day 7 PI, with a slight increase in viral load of 0.4 $\log_{10}$. On day 9 PI, the levels of vRNA for nocodazole-treated and untreated WNV-infected mice were similar, with a slight decrease in vRNA for the nocodazole-treated animals of 0.16 $\log_{10}$. This difference was statistically significant ($P = .003$) (Figure 2G, H).

In order to compare all collected tissues, we performed a product-limit survival function estimate to determine the incidence of vRNA in tissue or serum. This analysis measures a positive event, referring to vRNA in tissue or serum over the time of infection. The data determined that there exists a delay in infection following nocodazole treatment compared to the WNV treatment alone. Hence there is a 39% probability that a given CNS tissue will become infected following nocodazole treatment at any time point compared to a 75% probability that a CNS tissue would contain vRNA in the untreated WNV-infected mice (Figure 3).

The distribution of WNV antigens differed in the nocodazole-treated compared to untreated WNV-infected animals

In untreated WNV-infected animals, viral antigens were commonly found in the hippocampus, entorhinal cortex, and choroid plexus; however, this pattern of infection changed with nocodazole treatment

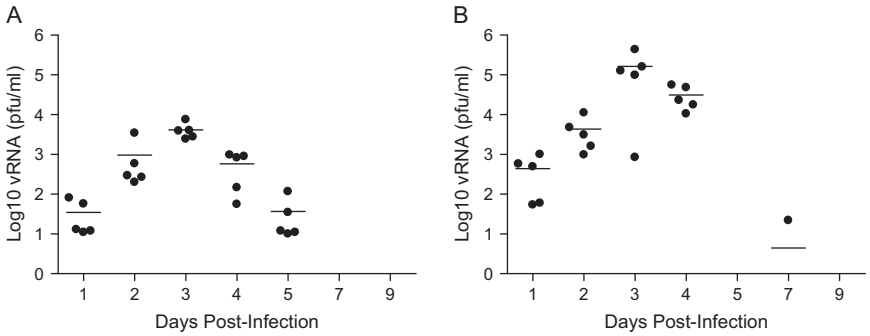

Figure 1 Scatter plots of the mean values of days post treatment represented by bars of WNV RNA (vRNA) in the serum of WNV-treated (**A**) and nocodazole-treated mice (**B**). Each time point is an average of $n = 5$ mice (ANOVA mixed model $P < .0001$).

(Hunsperger and Roehrig, 2006). The nocodazole-treated animals did not stain positive in the choroid plexus cells, implying different mechanisms of viral entry following treatment (Figure 4A and B). Whereas untreated WNV-infected animals commonly expressed viral antigens in the hippocampus region of the brain, nocodazole-treated mice did not express viral antigen in the hippocampus (Figure 4C and D). In addition, in the nocodazole-treated animals, the viral antigens were commonly expressed in the median eminence region of the brain and somatosensory cortex (Figure 4E and F).

Statistical analysis

An analysis of bivariate scrutiny revealed that nocodazole has a statically significant protective effect on the tissue of having viremia at all time points tested (risk ratio [RR] .51; 95% confidence interval [CI] 0.41, 0.065). Further analysis using a general linear model was performed using the log-transformed viremia as a dependent variable and treatment, time, and tissue as covariates, which yielded a $P < .0001$ for this model. In addition, a product limit survival test was performed, which demonstrated that tissue of mice treated with nocodazole had a statistically significant better chance to have ''survived'' viremia than the non–nocodazole-treated tissue ($P < .0001$) (Figure 3). Such differences behave the same over all tissue with the exception of the serum.

A mixed-model analysis with an unstructured covariance matrix using the subject within each point in time was carried out and resulted in a better fit for treatment effect of nocodazole. Comparisons of the least square difference between tissue types were statistically significant, with the exception of brainstem and spinal cord and between cerebellum and cortex.

Discussion

Flavivirus neuroinvasion of the CNS had been hypothesized to occur directly via the olfactory bulb or through a blood-brain barrier (BBB) breakdown (Monath *et al*, 1983). Another plausible route of viral neuroinvasion is via ART from peripheral sites to the CNS. The initial inoculation of the virus by the mosquito occurs in the dermal epithelium where the mosquito may probe up to 20 times in search for a blood meal (Ribeiro *et al*, 1985). The dermal epithelium is highly enervated by sensory neurons and highly exposed to infected saliva during the probing process, suggesting a route of infection for peripheral neurons. Evidence for ART of WNV has been obtained from neuropathological studies with WNV-infected humans (Fratkin *et al*, 2004; Smith *et al*, 2004). Moreover, high viral titers or sustained viremia in humans are not associated with neuroinvasion and not considered a mechanism of BBB breakdown (Biggerstaff and Petersen, 2002; Pealer *et al*, 2003).

This study used the microtubule inhibitor nocodazole to determine its effects following a WNV infection. Nocodazole is an antimitotic compound that disrupts microtubules by binding to β-tubulin and preventing the formation of interchain disulfide linkages (Luduena and Roach, 1991). This process results in the inhibition of microtubule dynamics and disruption of spindle function in addition to the fragmentation of the Golgi complex (Storrie and Yang, 1998). In normally dividing cells, nocodazole disrupts the cell cycle at the G2/M phase. However, because neurons are nondividing cells, nocodazole does not exert this effect. Nocodazole affects the immune system by preventing the phosphorylation of the T-cell antigen receptor, which decreases T-cells activity (Huby *et al*, 1998). Other known activities of nocodazole include activation of the c-Jun-N-terminal kinase/stress-activated protein kinase (JNK/SAPK) pathway and the induction of apoptosis in certain cell lines (Wang *et al*, 1998). In the neuronal system, nocodazole blocks axonal transport when tested in sensory neurons (Guan and Clark, 2006). In neurons, regions between the nucleus and the Golgi apparatus are unaffected by nocodazole treatment, suggesting that the replication and packaging of the virus remains intact. This is due to the fact that these regions of the neuron are composed of older, more stable microtubules, which are resistant to nocodazole treatment (Letourneau

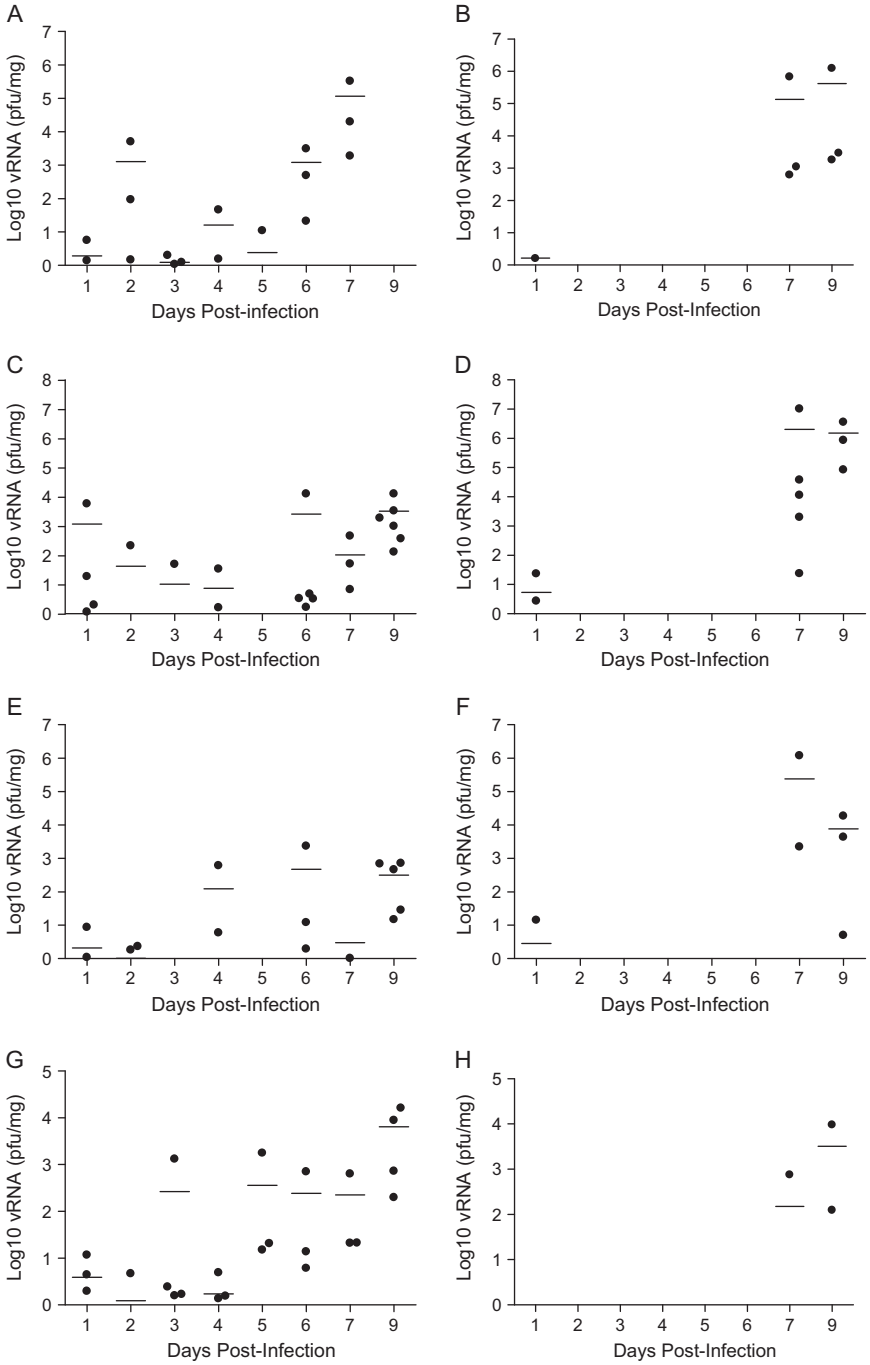

Figure 2 Scatter plots of the mean values of days post treatment represented by bars of WNV RNA detected in WNV-infected, untreated (**A, C, E,** and **G**), and WNV-infected, nocodazole-treated (**B, D, F,** and **H**) tissues: spinal cord (**A** and **B**; ANOVA mixed model $P = .01$); brain stem (**C** and **D**); cerebellum (**E** and **F**); and cortex (**G** and **H**; ANOVA mixed model $P = .003$). Each time point is an average of $n = 5$ mice. vRNA for days 5 and 6 were not measured for nocodazole-treated animals.

and Wire, 1995). However, the transport system, either retrograde or anterograde, would be most vulnerable to nocodazole treatment. We observed similar results in our studies, namely that sensory neurons were insensitive to nocodazole treatment and WNV replication and secretion were unaffected (Hunsperger and Roehrig, 2005). Viral antigens were restricted to the cell body and not found in the axonal regions of the neuron, suggesting a loss in ART of viral antigens following nocodazole treatment. Our studies utilized a well-characterized mouse model to determine the pathogenesis of WNV in the presence of nocodazole (Hunsperger and Roehrig, 2006).

Nocodazole increased the level of viremia in mice. Although the time of peak viremia in the blood did

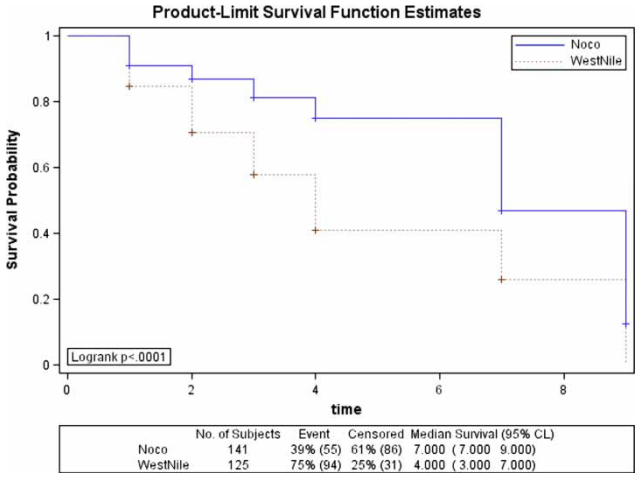

Figure 3 Product limit survival function estimates to determine the number of events (the probability that virus is present in any given tissue at any given time). Table below the graph demonstrates the number of events, censored and median survival with 95% confidence limits (CL).

not change for both treated and untreated mice, the titer of the virus in the serum of the nocodazole-treated mice increased on days 1 to 4 PI and this difference was statistically significant. Nocodazole may have compromised the immune system, perhaps demonstrating the importance of T-cell antigen receptor in viral replication. The expression of immunoglobulin G (IgG) antibodies against WNV did not change between nocodazole-treated and untreated mice, suggesting the B cells were unaffected by the nocodazole treatment (data not shown). Hence, the humoral immune response plays an important role in the initial viral replication as previously shown (Diamond *et al*, 2003; Halevy *et al*, 1994).

Viral RNA in the CNS was delayed for the nocodazole-treated animals and overall titers were greater than untreated animals. The levels of vRNA in the blood did not affect the CNS tissue levels, suggesting that viral load in the blood is not critical for neuroinvasion. In WNV-treated animals, the viral antigens were observed in the spinal cord on days 1 and 2 PI, implying an early infection of the CNS and later a clearance of the virus followed by reinfection. Nocodazole-treated animals did not have vRNA until day 7 PI in the spinal cord. Interestingly, the brainstem and the cerebellum had vRNA 1 day PI, but later there was clearance and expression of vRNA that peaked on day 7 PI and for the cerebellum decreased on day 9 PI. The delay in vRNA expression in the CNS may indicate that the virus replication is maintained in peripheral tissues such as the DRG and upon clearance of nocodazole, the virus is then capable of infecting the CNS. The DRG neurons of the PNS can harbor a persistent infection and maintain virus replication despite nocodazole treatment (Hunsperger and Roehrig, 2005). When nocodazole decreases below the threshold levels necessary for inhibition of viral transport via microtubules, the neurons transport the virus to the CNS. Because nocodazole has an inhibitory effect on the immune system by preventing the phosphorylation of T-cell antigen receptor and inhibiting its activity, this immune modulation may have increased vRNA in the CNS; however, we observed the opposite effect (Shrestha and Diamond, 2004).

Based on our data, WNV-treated animals were 75% more likely to harbor a CNS infection compared to nocodazole-treated mice (39%) (Figure 3). When examining the tissues using a mixed-model ANOVA analysis (which measured the vRNA in the tissue over time), we determined that the difference in vRNA among cortex, spinal cord, and serum were statistically significant. Therefore, viral entry in these tissues (spinal cord and cortex) was significantly blocked with nocodazole treatment. Once nocodazole was cleared from the animals and its effectiveness lost, alternate routes of viral infection was observed as shown in the histopathology results.

Previous pathology results of WNV in mice indicated that particular regions of the brain, including the choroid plexus, piriform cortex, or hippocampus, were sensitive to WNV infection and were most commonly found to harbor viral antigens in mice (Hunsperger and Roehrig, 2006). However, the histopathology results following nocodazole treatment suggest no involvement of these regions (choroid plexus, piriform cortex, or hippocampus) early in the infection (4 days PI). In addition, staining of WNV antigen was observed in the circumventricular organ (median eminence), which was not observed in WNV histopathology. Because these regions of the brain do not contain BBB, the increase in vRNA in the blood may account for this difference in viral antigen expression.

The studies presented here demonstrated that microtubule disruption with nocodazole alters WNV neuroinvasion. Treatment with nocodazole delayed viral entry into the CNS and increased viral load in the blood. In addition, viral antigen expression in the CNS was altered by the treatment, suggesting that peripheral virus replication is maintained and introduced into the CNS by peripheral means, such as the circumventricular organs where there is no BBB protection.

Materials and methods

Virus strain

The New York 1999 (NY99) strain of WNV used in these studies was obtained from the reference collection at the Division of Vector-Borne Infectious Diseases, Centers for Disease Control and Prevention (CDC). This WNV strain was isolated from an infected Chilean flamingo in the Bronx Zoo and was passaged once in suckling mice and twice in

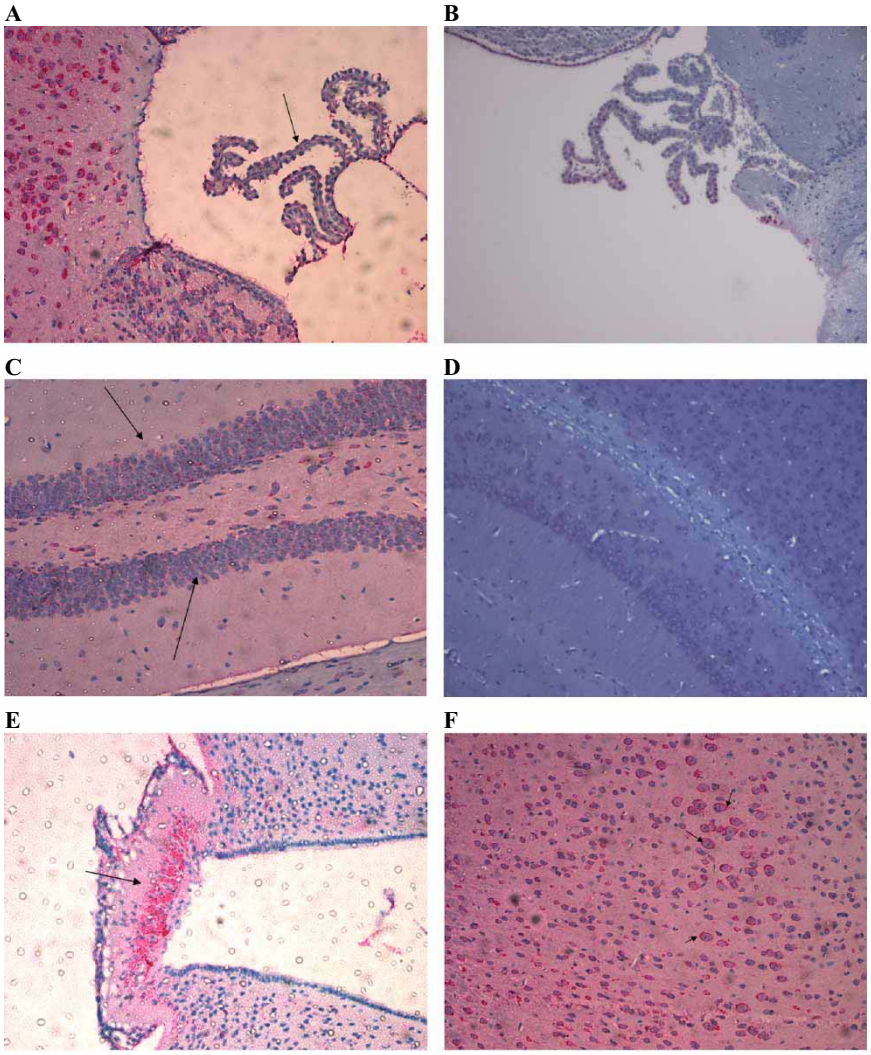

Figure 4 Immunohistochemistry of the (**A**) choroid plexus with no viral antigens present in nocodazole-treated animals (20×), indicated by the arrows, compared with (**B**) WNV-treated with viral antigens present; (**C**) hippocampus region demonstrating no viral antigens present in nocodazole-treated animals (400×) and (**D**) hippocampus of WNV-treated alone with viral antigens present (400×); (**E**) median eminence region of the brain demonstrating positive staining for viral antigen on day 7 post infection in nocodazole-treated animals (120×); (**F**) somatosensory cortex demonstrating positive staining for viral antigens on day 4 post infection of nocodazole-treated animals (200×).

Vero cells (Lanciotti *et al*, 1999). The NY99 strain of WNV is highly neurotropic (Beasley *et al*, 2002; Lanciotti *et al*, 2002).

Mouse footpad injection and nocodazole treatment
C57Bl/6J mice were obtained from Jackson laboratories at 6 weeks of age. The animals were anesthetized using isofluorane and infected with WNV via a footpad injection with approximately 1200 plaque-forming units (PFU) per animal (Hunsperger and Roehrig, 2006). The animals in the nocodazole treatment group received 5 mg/kg of nocodazole (Sigma, St Louis, MO), the effective dose for inhibition of tumor growth in mice, via intraperitoneal injection (IP) 1 h prior to infection with WNV (Lee *et al*, 2003). Viral stock solution for the infection was diluted to the appropriate concentration using 1% fetal bovine serum in sterile phosphate-buffered saline (PBS). Tissue samples were harvested from spinal cord (SC) and brain on days 1 through 9 (SC WNV day 9 and nocodazole-treated animals days 5 and 6 were not measured). This tissue was analyzed using immunohistochemistry for viral antigen expression and TaqMan analysis for the presence of viral RNA. Serum samples were obtained during the course of the infection to determine the viremic state of the animals. These samples were analyzed using TaqMan to determine the viral RNA present in the serum.

Viral RNA isolation and quantitation using TaqMan analyses
Viral RNA was isolated from virus seed and serum samples using a QiaAmp viral RNA kit (Qiagen, Valencia, CA). Tissue samples from the nervous

system, including brain and spinal cord, were weighed and homogenized using a dounce tissue grinder in the presence of lysis buffer from the Qiagen RNeasy kit according to manufacturer's instructions. The samples were frozen at −70°C for later processing. WNV reverse transcriptase–polymerase chain reaction (RT-PCR) primers used to determine the viral RNA content in the tissue samples were previously described. Briefly, the forward envelope primer was designed from WNV genome positions 1160 to 1180, the reverse envelope primer was designed from genome positions 1209 to 1229, and the probe was designed from genome positions 1186 to 1207. Sequences for these primers can be obtained from previous publications. Genome position was determined according to the WNV NY99 complete genome sequence. The detection limit of this assay is 0.1 PFU; values below 0.1 PFU were considered negative. Previous studies using human brain tissue determined that recovery of virus particles from the tissue sample was 100% accurate when compared to positive serological results (Lanciotti *et al*, 2000, 2002).

Five microliters of the total RNA extracted from each sample was analyzed by TaqMan assay. The reaction included 50 pmol of each primer and 10 pmol of the FAM- and TAMRA-labeled probe using the one-step RT-PCR master mix (PE Applied Biosystems, Foster City, CA) in a 50-µl reaction volume. The samples were cycled 45 times for amplification in an ABI Prism 7700 Sequence Detection System instrument (PE Applied Biosystems) according to manufacturer's suggested protocol for TaqMan assay RT-PCR cycling conditions. A standard curve determined from the viral seed NY99 was compared to a standard plaque assay from the same samples to calculate PFU/ml or PFU/mg based on cycle threshold values (C_T). Negative controls included non–template-uninfected animal tissue and serum.

Indirect immunofluorescence antibody assay

Blood samples were tested for the presence of WNV-reactive antibodies for each time point. The blood samples were centrifuged in microfuge plasma separator tubes and plasma samples were diluted 1:2 in PBS. The samples were added to a slide containing acetone-fixed WNV-infected Vero cells. Following incubation at 37°C, the slides were washed three times with PBS and treated with a secondary antibody anti-mouse immunoglobulin G (IgG) conjugated to fluorescein isothiocyanate (FITC) (Jackson Laboratories) diluted in PBS at 1:100. Visual analysis of the presence of fluorescence for each sample was used as an endpoint. Controls included plasma from uninfected animals and PBS alone.

Immunohistochemistry

Brain samples of nocodazole-treated WNV-infected mice were harvested and immersion fixed in 10% formalin at various time points (1 to 9 days PI) (Fisher Scientific). The samples were paraffin embedded and coronal sections of 5 µm were mounted on glass slides. The tissue was processed using a BenchMark LTIHC/ISH histochemistry staining machine utilizing the XT Enhanced V-Red V.1 standardized staining protocol (Ventana, Tucson, AZ). Following deparaffinization and rehydration of sample, the tissue was blocked with 2% goat serum (GS) in PBS for 20 minutes and then probed with the primary polyclonal antibody against WNV (Ar248; CDC reference collection) for 1 h, followed by three washes with PBS. The sections were probed with a secondary antibody consisting of anti-mouse IgG conjugated to peroxidase (Jackson Laboratories). All antibody solutions were diluted in 1% GS in PBS. Fast red (which yields a red precipitate) was used to visualize viral antigens in tissue samples, which were then counterstained with hemotoxyline. Analysis of the data was performed using the stereotaxic coordinate map of the mouse brain (Franklin and Paxinos, 1977).

Statistical analysis

Statistical analysis used for this study included an analysis of bivariate scrutiny, general linear model, a product limit survival test, and mixed-model analysis with an unstructured covariance matrix.

Declaration of interest: The authors report no conflicts of interest. The authors alone are responsible for the content and writing of the paper.

References

Anderson JF, Andreadis TG, Vossbrinck CR, Tirrell S, Wakem EM, French RA, Garmendia AE, Van Kruiningen HJ (1999). Isolation of West Nile virus from mosquitoes, crows, and a Cooper's hawk in Connecticut. *Science* **286:** 2331–2333.

Beasley DW, Li L, Suderman MT, Barrett AD (2002). Mouse neuroinvasive phenotype of West Nile virus strains varies depending upon virus genotype. *Virology* **296:** 17–23.

Biggerstaff BJ, Petersen LR (2002). Estimated risk of West Nile virus transmission through blood transfusion during an epidemic in Queens, New York City. *Transfusion* **42:** 1019–1026.

Briese T, Jia XY, Huang C, Grady LJ, Lipkin WI (1999). Identification of a Kunjin/West Nile-like flavivirus in brains of patients with New York encephalitis. *Lancet* **354:** 1261–1262.

Brinton MA (2002). The molecular biology of West Nile Virus: a new invader of the western hemisphere. *Annu Rev Microbiol* **56:** 371–402.

Diamond MS, Shrestha B, Marri A, Mahan D, Engle M (2003). B cells and antibody play critical roles in the immediate defense of disseminated infection by West Nile encephalitis virus. *J Virol* **77:** 2578–2586.

Doron SI, Dashe JF, Adelman LS, Brown WF, Werner BG, Hadley S (2003). Histopathologically proven poliomyelitis with quadriplegia and loss of brainstem function due to West Nile virus infection. *Clin Infect Dis* **37:** e74–e77.

Franklin KB, Paxinos G (1977). *The mouse brain in stereotaxic coordinates*. San Diego: Academic Press.

Fratkin JD, Leis AA, Stokic DS, Slavinski SA, Geiss RW (2004). Spinal cord neuropathology in human West Nile virus infection. *Arch Pathol Lab Med* **128:** 533–537.

Guan X, Clark GA (2006). Essential role of somatic and synaptic protein synthesis and axonal transport in long-term synapse-specific facilitation at distal sensorimotor connections in Aplysia. *Biol Bull* **210:** 238–254.

Halevy M, Akov Y, Ben-Nathan D, Kobiler D, Lachmi B, Lustig S (1994). Loss of active neuroinvasiveness in attenuated strains of West Nile virus: pathogenicity in immunocompetent and SCID mice. *Arch Virol* **137:** 355–370.

Huby RD, Weiss A, Ley SC (1998). Nocodazole inhibits signal transduction by the T cell antigen receptor. *J Biol Chem* **273:** 12024–12031.

Hunsperger E, Roehrig JT (2005). Characterization of West Nile viral replication and maturation in peripheral neurons in culture. *J NeuroVirol* **11:** 11–22.

Hunsperger EA, Roehrig JT (2006). Temporal analyses of the neuropathogenesis of a West Nile virus infection in mice. *J NeuroVirol* **12:** 129–139.

Lanciotti RS, Ebel GD, Deubel V, Kerst AJ, Murri S, Meyer R, Bowen M, McKinney N, Morrill WE, Crabtree MB, Kramer LD, Roehrig JT (2002). Complete genome sequences and phylogenetic analysis of West Nile virus strains isolated from the United States, Europe, and the Middle East. *Virology* **298:** 96–105.

Lanciotti RS, Kerst AJ, Nasci RS, Godsey MS, Mitchell CJ, Savage HM, Komar N, Panella NA, Allen BC, Volpe KE, Davis BS, Roehrig JT (2000). Rapid detection of West Nile virus from human clinical specimens, field-collected mosquitoes, and avian samples by a TaqMan reverse transcriptase-PCR assay. *J Clin Microbiol* **38:** 4066–4071.

Lanciotti RS, Roehrig JT, Deubel V, Smith J, Parker M, Steele K, Crise B, Volpe KE, Crabtree MB, Scherret JH, Hall RA, MacKenzie JS, Cropp CB, Panigrahy B, Ostlund E, Schmitt B, Malkinson M, Banet C, Weissman J, Komar N, Savage HM, Stone W, McNamara T, Gubler DJ (1999). Origin of the West Nile virus responsible for an outbreak of encephalitis in the northeastern United States. *Science* **286:** 2333–2337.

Lee WS, Chen RJ, Wang YJ, Tseng H, Jeng JH, Lin SY, Liang YC, Chen CH, Lin CH, Lin JK, Ho PY, Chu JS, Ho WL, Chen LC, Ho YS (2003). In vitro and in vivo studies of the anticancer action of terbinafine in human cancer cell lines: G0/G1 p53-associated cell cycle arrest. *Int J Cancer* **106:** 125–137.

Leis AA, Fratkin J, Stokic DS, Harrington T, Webb RM, Slavinski SA (2003). West Nile poliomyelitis. *Lancet Infect Dis* **3:** 9–10.

Letourneau PC, Wire JP (1995). Three-dimensional organization of stable microtubules and the Golgi apparatus in the somata of developing chick sensory neurons. *J Neurocytol* **24:** 207–223.

Luduena RF, Roach MC (1991). Tubulin sulfhydryl groups as probes and targets for antimitotic and antimicrotubule agents. *Pharmacol Ther* **49:** 133–152.

Monath TP, Cropp CB, Harrison AK (1983). Mode of entry of a neurotropic arbovirus into the central nervous system. Reinvestigation of an old controversy. *Lab Invest* **48:** 399–410.

Nash D, Mostashari F, Fine A, Miller J, O'Leary D, Murray K, Huang A, Rosenberg A, Greenberg A, Sherman M, Wong S, Layton M (2001). The outbreak of West Nile virus infection in the New York City area in 1999. *N Engl J Med* **344:** 1807–1814.

Pealer LN, Marfin AA, Petersen LR, Lanciotti RS, Page PL, Stramer SL, Stobierski MG, Signs K, Newman B, Kapoor H, Goodman JL, Chamberland ME (2003). Transmission of West Nile virus through blood transfusion in the United States in 2002. *N Engl J Med* **349:** 1236–1245.

Ribeiro JM, Rossignol PA, Spielman A (1985). Aedes aegypti: model for blood finding strategy and prediction of parasite manipulation. *Exp Parasitol* **60:** 118–132.

Samuel MA, Wang H, Siddharthan V, Morrey JD, Diamond MS (2007). Axonal transport mediates West Nile virus entry into the central nervous system and induces acute flaccid paralysis. *Proc Natl Acad Sci U S A* **104:** 17140–17145.

Shrestha B, Diamond MS (2004). Role of CD8+ T cells in control of West Nile virus infection. *J Virol* **78:** 8312–8321.

Smith RD, Konoplev S, DeCourten-Myers G, Brown T (2004). West Nile virus encephalitis with myositis and orchitis. *Hum Pathol* **35:** 254–258.

Smithburn K, Hughes T, Burke A (1940). A neurotropic virus isolated from the blood of a native of Uganda. *Am J Trop Med Hyg* **20:** 471–492.

Storrie B, Yang W (1998). Dynamics of the interphase mammalian Golgi complex as revealed through drugs producing reversible Golgi disassembly. *Biochim Biophys Acta* **1404:** 127–137.

Wang TH, Wang HS, Ichijo H, Giannakakou P, Foster JS, Fojo T, Wimalasena J (1998). Microtubule-interfering agents activate c-Jun N-terminal kinase/stress-activated protein kinase through both Ras and apoptosis signal-regulating kinase pathways. *J Biol Chem* **273:** 4928–4936.

This paper was first published online on iFirst on 13 May 2009.